Electronic Journal of Biotechnology 81 (2026) 100712

Contents lists available at ScienceDirect

Electronic Journal of Biotechnology

journal homepage: www.elsevier.com/locate/ejbt

Research article

Periodontal ligament stem cell-derived exosomes promote alveolar bone defect repair in periodontitis by mediating M2 macrophage polarization via regulation of the SEMA4D/PLXNB1 axis ☆

YanZong Yang [a,b], ChunBo Zhang [a,b,*]

[a] Department of Stomatology, The First Affiliated Hospital of Xiamen University, Xiamen City, Fujian Province, China
[b] School of Medicine, Xiamen University, Xiamen City, Fujian Province, China

GRAPHICAL ABSTRACT

Periodontal ligament stem cell-derived exosomes promote alveolar bone defect repair in periodontitis by mediating M2 macrophage polarization via regulation of the SEMA4D/PLXNB1 axis.

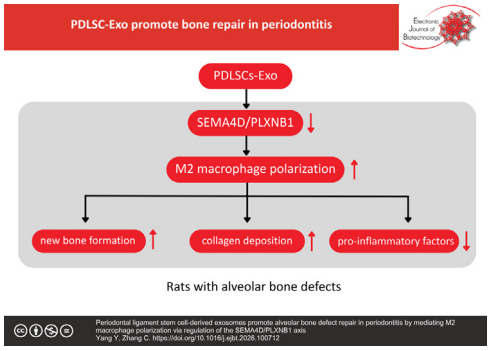

ARTICLE INFO

Article history:
Received 3 September 2025
Accepted 23 January 2026
Available online 8 April 2026

Keywords:
Alveolar bone loss
Bone regeneration
Macrophage polarization
Periodontal ligament
Periodontitis
Plexin B1
Semaphorin 4D
Signal transduction

ABSTRACT

Background: Periodontitis is a chronic inflammatory disease characterized by progressive alveolar bone loss. This study explored the role of exosomes derived from periodontal ligament stem cells (PDLSCs-Exo) in repairing alveolar bone defects in periodontitis.
Results: PDLSCs-Exo significantly promoted new bone formation and collagen deposition in the defect area while reducing pro-inflammatory factors and enhancing M2 macrophage polarization. The knockdown of semaphorin 4D (SEMA4D) or plexin B1 (PLXNB1) further enhanced exosome-mediated repair, whereas their overexpression attenuated it. Additionally, the upregulation of PLXNB1 reversed the reparative effects of SEMA4D downregulation on alveolar bone defects in periodontitis.
Conclusions: PDLSCs-Exo promotes M2 macrophage polarization by inhibiting the SEMA4D/PLXNB1 axis, alleviating local inflammation and accelerating alveolar bone defect repair in periodontitis. This finding provides a novel theoretical basis for the clinical treatment of periodontitis-related alveolar bone defects and identifies potential therapeutic targets for improving the efficacy of bone defect repair.

☆ Audio abstract available in Supplementary material.
Peer review under responsibility of Pontificia Universidad Católica de Valparaíso.
* Corresponding author.
E-mail address: zhangchunbo_zc@hotmail.com (C. Zhang).

https://doi.org/10.1016/j.ejbt.2026.100712

Sprague-Dawley
Stem cells
Tissue repair

How to cite: Yang Y, Zhang C. Periodontal ligament stem cell-derived exosomes promote alveolar bone defect repair in periodontitis by mediating M2 macrophage polarization via regulation of the SEMA4D/PLXNB1 axis. Electron J Biotechnol 2026;81. https://doi.org/10.1016/j.ejbt.2026.100712.

1. Introduction

Periodontitis ranks as the second most prevalent oral disorder globally, with its incidence rate surpassing 40% [1]. Periodontitis is a chronic inflammatory disease that progressively destroys the periodontal supporting structures, leading to alveolar bone resorption and eventual tooth exfoliation [2]. Current understanding of its pathogenesis indicates that impaired osteogenic capacity and disrupted osteoimmune homeostasis represent the primary obstacles to effective alveolar bone regeneration [3]. Current clinical interventions, such as removal of local irritants, antibiotic therapy, and surgical bone procedures, are primarily aimed at controlling infection and restoring structural integrity. However, these approaches fall short in simultaneously promoting new bone formation and reestablishing a pro-regenerative immune environment [4]. Therefore, developing novel treatment strategies that not only enhance osteogenesis but also correct immune imbalances is critical for achieving effective in situ reconstruction of alveolar bone in periodontal disease.

Periodontal ligament stem cells (PDLSCs) represent a population of multipotent mesenchymal stem cells that hold considerable promise for regenerating periodontal tissues, owing to their inherent abilities of self-renewal and capacity for multi-lineage differentiation [5,6,7]. In recent years, exosomes derived from stem cells have attracted significant attention as key mediators of intercellular communication. They carry various bioactive molecules (such as proteins and nucleic acids) and exhibit immunomodulatory and tissue regenerative capabilities [8,9,10,11,12]. Emerging evidence suggests that periodontal ligament stem cell-derived exosomes (PDLSCs-Exo) may exhibit therapeutic potential for promoting alveolar bone regeneration in periodontitis [13,14,15,16].

Macrophages serve as pivotal regulators in periodontal inflammation and subsequent tissue regeneration processes. M1 macrophages are primarily involved in pro-inflammatory responses and exacerbate alveolar bone loss, whereas M2 macrophages possess anti-inflammatory and pro-repair functions [17,18,19]. Therefore, modulating macrophage polarization toward the M2 phenotype is considered a promising strategy for treating periodontitis, particularly in promoting alveolar bone regeneration [20,21,22].

This study aims to investigate the role and underlying mechanisms of PDLSCs-Exo in the repair of alveolar bone defects in periodontitis. Using a rat model of periodontitis with alveolar bone defects, the effects of PDLSCs-Exo were evaluated on alveolar bone regeneration, levels of pro-inflammatory cytokines, and macrophage polarization through histological, immunohistochemical (IHC), enzyme-linked immunosorbent assay (ELISA), and molecular biological techniques. Previous studies have shown that semaphorin 4D (SEMA4D) is upregulated in osteoporosis, and downregulation of SEMA4D promotes osteoblast activity [23]. Specifically, this study focuses on the regulatory role of the SEMA4D and its receptor plexin B1 (PLXNB1) axis in PDLSCs-Exo-mediated M2 macrophage polarization and alveolar bone defect repair, which could provide new therapeutic targets and strategies for treating periodontitis.

2. Materials and methods

2.1. Isolation, culture, and identification of PDLSCs

All animal procedures were approved by the Institutional Animal Care and Use Committee and were performed in accordance with its guidelines. Seventy-two five-week-old male Sprague-Dawley (SD) rats were obtained from the Guangdong Medical Laboratory Animal Center. The animals were housed under standardized conditions (temperature of 25 ± 1°C, humidity of 55–65%, and a 12 h light/dark cycle) with ad libitum access to food and water. The rats were acclimatized for one week before the experiments.

Periodontal ligament (PDL) tissues were aseptically harvested from the first and second molars of six SD rats following gingival tissue excision. The collected tissue specimens were then subjected to enzymatic digestion for 60 min at 37°C with gentle agitation, using a solution containing 3 mg/mL collagenase type I and 4 mg/mL dispase II [24]. Subsequently, the resulting cell suspension was filtered through a 70 μm nylon mesh and seeded at a low density (1 × 103 to 1 × 104 cells/cm^2) into culture dishes. The growth medium consisted of Dulbecco's Modified Eagle Medium (DMEM; Gibco, USA) supplemented with 10% fetal bovine serum (FBS; Gibco) and 1% penicillin–streptomycin (Hyclone, USA).

After a 10 d culture period, the cells were fixed with 4% paraformaldehyde (Servicebio, China). Colony formation was assessed by staining with methylene blue (Sigma-Aldrich, USA), and cell clusters containing 50 or more cells were identified as a single colony. For all subsequent experimental procedures, cells from passages 2 to 5 were utilized.

Flow cytometry was employed to analyze the surface antigen expression of PDLSCs. In brief, the digested PDLSCs were stained with the following anti-rat antibodies: integrin beta-1 (CD29, PE-conjugated; BioLegend, USA), Thy-1 cell surface antigen (CD90, PE-conjugated; BioLegend), and melanoma cell adhesion molecule (CD146, PE-conjugated; BioLegend) as positive markers for mesenchymal stem cells (MSCs); integrin alpha-M (CD11b, FITC-conjugated; BioLegend), hematopoietic progenitor cell antigen (CD34, FITC-conjugated; BioLegend), and protein tyrosine phosphatase, receptor type, C (CD45, Alexa Fluor 647-conjugated; BioLegend) as negative hematopoietic lineage markers. The stained cells were then analyzed using a flow cytometer (Becton Dickinson, USA).

To evaluate osteogenic differentiation capacity, cells were cultured under osteoinductive conditions according to established methods [25]. Mineralized matrix deposition was quantified using Alizarin Red S staining (Cyagen, USA). For adipogenic differentiation, cells were exposed to a differentiation cocktail consisting of 1 μM dexamethasone, 0.5 mM 3-isobutyl-1-methylxanthine, 200 μM indomethacin, and 10 μg/mL insulin. All reagents were obtained from Sigma-Aldrich, with the exception of insulin (Gibco). Following 14 d of induction, intracellular lipid droplet formation was assessed by Oil Red O staining (Sigma-Aldrich) after fixation with 4% paraformaldehyde.

2.2. Cell transfection

For overexpressing SEMA4D and PLXNB1, full-length sequences were synthesized and subcloned into the pcDNA3.1 vector, with the empty pcDNA3.1 vector used as the negative control (NC). For inhibiting SEMA4D and PLXNB1, specific small interfering RNAs (siRNAs) were synthesized, with a non-targeting siRNA (si-NC) serving as the NC. Cell transfection was performed using Lipotransfectamine 3000 (Thermo Fisher Scientific, USA) according to the manufacturer's instructions. Exosomes were isolated from PDLSCs 48 h after transfection.

2.3. Isolation and Identification of PDLSCs-Exo

Exosomes were isolated using differential ultracentrifugation [26]. Briefly, PDLSCs at passage 3 from SD rats were maintained in 10 cm culture dishes. Cells were grown in complete medium until approximately 80% confluence was attained, after which the medium was replaced with serum-free medium for an additional 48 h period. The conditioned medium was collected and subjected to centrifugation at 300 × *g* for 15 min at 4°C. Following removal of the pellet, the supernatant was further centrifuged at 3,000 × *g* for 15 min. The resulting supernatant was then ultracentrifuged at 100,000 × *g* twice, with each run lasting 70 min. Protein concentration of the isolated exosomes was measured using a Bicinchoninic Acid (BCA) Protein Assay Kit (Thermo Fisher Scientific), yielding a total protein amount of 630 μg. The exosome pellet was resuspended in ice-cold phosphate-buffered saline (PBS) and stored at −80°C until further analysis.

The morphology of exosomes was observed using transmission electron microscopy (TEM; Philips TECNAI 20, Netherlands). Particle size distribution was analyzed by nanoparticle tracking analysis (NTA). Expression of exosomal markers CD9 (Proteintech, China), CD63 (Proteintech), and TSG101 (Proteintech) was detected by Western blot.

2.4. Preparation of PDLSCs-exo composite hydrogel

A nanocomposite hydrogel was prepared by mixing 5% gelatin (Sigma, USA) dissolved in ddH_2O at 37°C with a ddH_2O solution containing 10% Laponite® (Nanocor, China) [27]. PDLSCs-Exo were loaded into the hydrogel at a 1:1 vol ratio at 4°C. The controlled release capability of the hydrogel was evaluated through a release assay. Briefly, 500 μL of the PDLSCs-Exo-hydrogel mixture was aliquoted into a microcentrifuge tube, and 200 μL of PBS was gently layered on top. Following incubation at 37°C for 24 h, the supernatant was collected, and the total protein content released was quantified using a BCA kit (Thermo Fisher Scientific). Subsequently, the supernatant was replaced with 200 μL of fresh PBS, and the procedure was repeated daily for 28 d.

2.5. Establishment of a rat model of periodontitis with alveolar bone defects

In dental research, the rat experimental periodontitis model induced by molar ligation is widely used to investigate the pathological mechanisms of periodontitis. Ligating the cervix of rat molars leads to plaque accumulation, periodontal inflammation, and alveolar bone resorption, which closely resemble the manifestations of human periodontitis [28,29,30,31]. A periodontitis model was constructed in SD rats (n = 66) according to previously reported methods [32]. Following anesthesia with intraperitoneal sodium pentobarbital (60 mg/kg; Sigma-Aldrich), 5-0 silk sutures were placed around the cervical region of maxillary right second molars. After 3 weeks, the ligatures were taken out, and food residues, plaque, and calculus in the periodontal area were completely cleaned. To examine the impact of PDLSCs-Exo on repairing periodontal bone defects, a standardized alveolar bone defect with a diameter and depth of 3 mm was made on the palatal side of the maxillary right second molar in periodontitis rats using a dental drill [33]. During the procedure, continuous saline irrigation and intermittent low speed drilling were applied to minimize thermal injury [34]. Rats with alveolar bone defects were divided into the following 11 groups (n = 6 per group): Control (no treatment), Hydrogel (hydrogel treatment), Hydrogel + Exo (PDLSCs-Exo composite hydrogel treatment), Hydrogel + Exo-si-NC (PDLSCs-Exo-si-NC composite hydrogel treatment), Hydrogel + Exo-si-SEMA4D (PDLSCs-Exo-si-SEMA4D composite hydrogel treatment), Hydrogel + Exo-si-PLXNB1 (PDLSCs-Exo-si-PLXNB1 composite hydrogel treatment), Hydrogel + Exo-pcDNA3.1-NC (PDLSCs-Exo-pcDNA3.1-NC composite hydrogel treatment), Hydrogel + Exo-pc DNA3.1-SEMA4D (PDLSCs-Exo-pcDNA3.1-SEMA4D composite hydrogel treatment), Hydrogel + Exo-pcDNA3.1-PLXNB1 (PDLSCs-Exo-pcDNA3.1-PLXNB1 composite hydrogel treatment), Hydrogel + Exo-si-SEMA4D + pcDNA3.1-NC (PDLSCs-Exo-si-SEM A4D + pcDNA3.1-NC composite hydrogel treatment), and Hydrogel + Exo-si-SEMA4D + pcDNA3.1-PLXNB1 (PDLSCs-Exo-si-S EMA4D + pcDNA3.1-PLXNB1 composite hydrogel treatment). Penicillin at 10,000 U/day was injected intraperitoneally for 3 d to prevent infection. All rats were euthanized after 4 weeks of treatment.

2.6. Biochemical analysis

The concentrations of specific biochemical markers in serum were quantified using established commercial assay kits and automated instrumentation. Creatine kinase-MB (CK-MB) and cardiac troponin I (cTnI) levels were determined employing corresponding commercial kits (Nanjing Jiancheng, China) in strict accordance with the provided protocols. Concurrently, aspartate aminotransferase (AST) and alanine aminotransferase (ALT) activities in serum were analyzed utilizing a Beckman automatic biochemical analyzer (Roche, Germany). Furthermore, renal function parameters were assessed by measuring serum creatinine (Scr) and blood urea nitrogen (BUN) concentrations. The Scr level was evaluated with a colorimetric technique, while BUN was quantified using a dedicated creatinine assay kit (Nanjing Jiancheng), with both procedures adhering meticulously to the manufacturers' instructions.

2.7. Histological analysis

The maxillary right jaw samples were fixed in 4% paraformaldehyde, decalcified in 10% ethylenediaminetetraacetic acid, dehydrated through a graded ethanol series, and embedded in paraffin. Sections were cut at a thickness of 5 μm. Hematoxylin and eosin (H&E; Sigma) staining and Masson's trichrome (Sigma) staining were performed according to the manufacturers' instructions.

IHC staining was carried out as previously described [35]. Briefly, sections were deparaffinized, rehydrated, and subjected to antigen retrieval. The sections were incubated with primary antibodies against iNOS (1:200; Servicebio, China) or CD206 (1:200; Servicebio, China) at 4°C overnight, followed by incubation with secondary antibodies at room temperature for 1 h. Visualization was performed using diaminobenzidine (DAB; Servicebio, China), and the sections were counterstained with hematoxylin (Servicebio, China). Finally, the stained sections were observed under a microscope (Olympus, Japan).

2.8. ELISA

Commercial ELISA kits (Shanghai Enzyme-linked Biotechnology Co., Ltd., China) were utilized to determine the serum concentra-

tions of TNF-α, IL-1β, and IL-6 in rats, following the manufacturer's protocols.

2.9. Real-time quantitative polymerase chain reaction (RT-qPCR)

Total RNA was extracted from samples using Trizol reagent (Invitrogen, USA). Subsequent cDNA synthesis was performed following the manufacturer's protocol with a commercial reverse transcription kit (Funeng, China). Quantitative real-time PCR assays were then carried out on the resulting cDNA templates using a SYBR Green PCR kit (Funeng). The thermal cycling protocol comprised an initial denaturation step at 95°C for 30 s, followed by 40 cycles of denaturation at 95°C for 5 s and a combined annealing/extension step at 60°C for 30 s. Glyceraldehyde-3-phosphate dehydrogenase (GAPDH) was used as the endogenous control gene to normalize target gene expression. The relative expression levels of the target genes were calculated employing the comparative $2^{-\Delta\Delta Ct}$ method. All primer sequences utilized in this study are listed in Table 1.

2.10. Western blot

Total protein was extracted using radioimmunoprecipitation assay lysis buffer (Beyotime, China), and protein concentration was determined using a BCA assay kit (Thermo Fisher Scientific). Protein samples were separated by 10% sodium dodecyl sulfate–polyacrylamide gel electrophoresis and subsequently transferred onto polyvinylidene fluoride membranes (Millipore). Following a 1 h blocking step with 5% skim milk, the membranes were incubated with primary antibodies overnight at 4°C. After washing, the membranes were incubated with horseradish peroxidase-conjugated secondary antibodies (1:2000; Abcam) for 2 h at room temperature. Protein bands were visualized using an enhanced chemiluminescence substrate (Beyotime) and imaged with a chemiluminescence detection system. The primary antibodies used included those against SEMA4D (1:600; ABclonal Technology, China), PLXNB1 (1:600; Proteintech Group, Inc., USA), and GAPDH (1:1000; Abcam).

2.11. Co-Immunoprecipitation (Co-IP)

PDLSCs were lysed in Pierce IP Lysis Buffer (Thermo Fisher Scientific). The lysates were incubated overnight at 4°C with anti-SEMA4D antibody or control IgG. Immune complexes were captured using Protein A/G agarose beads (Thermo Fisher Scientific) for 4 h, washed and then analyzed by Western blot.

2.12. Statistical analysis

All data are presented as mean ± standard deviation. Statistical evaluations were conducted using Statistical Package for the Social Sciences 22.0 software. For comparisons between two groups, Student's *t*-test was applied, while differences among multiple groups were analyzed by one-way analysis of variance with subsequent Tukey's test. A value of $p < 0.05$ was considered statistically significant.

Table 1
Primer Sequences for RT-qPCR.

Gene	Sequence
SEMA4D	F: 5′-CGGAGAGGTAGGTCTGGTGA-3′ R: 5′-GTTAAGGCACTCCGTCTGCT-3′
PLXNB1	F: 5′-CGAGGCGGAGGAGTGGATGG-3′ R: 5′-CGAGGCTGGACAGGAGGATGAG-3′
GAPDH	F: 5′-GCTGAGTATGTCGTGGAGT-3′ R: 5′-GTTCACACCCATCACAAAC-3′

3. Results

3.1. Isolation and Identification of PDLSCs

After 10 d of low-density culture, cells isolated from the rat periodontal ligament formed distinct clonal clusters (Fig. 1A). The multipotent differentiation potential characteristic of mesenchymal stem cells was evaluated by osteogenic and adipogenic induction assays. Alizarin Red S staining confirmed mineralization, and Oil Red O staining identified lipid droplet accumulation (Fig. 1B, C). Flow cytometric analysis showed a surface marker profile typical of mesenchymal stem cells: positive for CD29, CD90, and CD146, and negative for CD11b, CD34, and CD45 (Fig. 1D). Collectively, these results confirm that the isolated cells exhibit defining properties of mesenchymal stem cells and are therefore identified as PDLSCs [36].

3.2. Isolation and identification of PDLSCs-exo

Exosomes were isolated from the supernatant of cultured PDLSCs and subsequently characterized. Transmission electron microscopy showed that the vesicles displayed a characteristic cup-shaped or spherical morphology (Fig. 2A). Nanoparticle tracking analysis indicated that their size distribution was predominantly between 90 and 150 nm (Fig. 2B). Western blot analysis confirmed the presence of the exosomal surface markers CD9, CD63, and TSG101 (Fig. 2C). Together, these results demonstrate the successful isolation of exosomes from PDLSC cultures.

3.3. PDLSCs-exo promote the repair of alveolar bone defects in periodontitis

A nanocomposite hydrogel was used to deliver PDLSCs-Exo locally for the evaluation of their therapeutic effect on alveolar bone defects in periodontitis. The encapsulation efficiency of PDLSCs-Exo within the hydrogel reached 92% (Fig. 3A). The cumulative release profile indicated that 44.50% of the exosomes were released by day 7, which increased to 77.10% by day 28 (Fig. 3B), demonstrating that the nanocomposite hydrogel acted as an effective sustained-release carrier. Biosafety assessment of the Hydrogel + Exo formulation was conducted by measuring serum biomarkers of cardiac (cTnI, CK MB), hepatic (ALT, AST), and renal (BUN, Scr) function. No significant abnormalities were observed in any of the measured biomarkers (Fig. S1), confirming its favorable biosafety profile. Histological evaluation via H&E staining indicated greater new bone formation in the alveolar bone defect sites of the Hydrogel + Exo group than in the control group (Fig. 3C). Correspondingly, Masson's trichrome staining displayed enhanced collagen deposition in the treated defect areas (Fig. 3D). Immunohistochemical analysis revealed a decrease in iNOS-positive cells and an increase in CD206-positive cells in the Hydrogel + Exo group (Fig. 3E, F), which supports the role of PDLSCs-Exo in promoting M2 macrophage polarization. Additionally, ELISA results demonstrated significantly lower serum concentrations of the pro-inflammatory cytokines TNF α, IL 1β, and IL 6 following treatment (Fig. 3G, H, I).

3.4. Downregulation of SEMA4D or PLXNB1 enhances the therapeutic effect of PDLSCs-exo on alveolar bone defect repair in periodontitis

Reduced expression of SEMA4D and its receptor PLXNB1 was observed in the Hydrogel + Exo group, as evidenced by RT qPCR and Western blot analyses (Fig. 4A, B). To investigate the functional role of these proteins, siRNA-mediated knockdown of SEMA4D or PLXNB1 was performed in PDLSCs prior to exosome isolation.

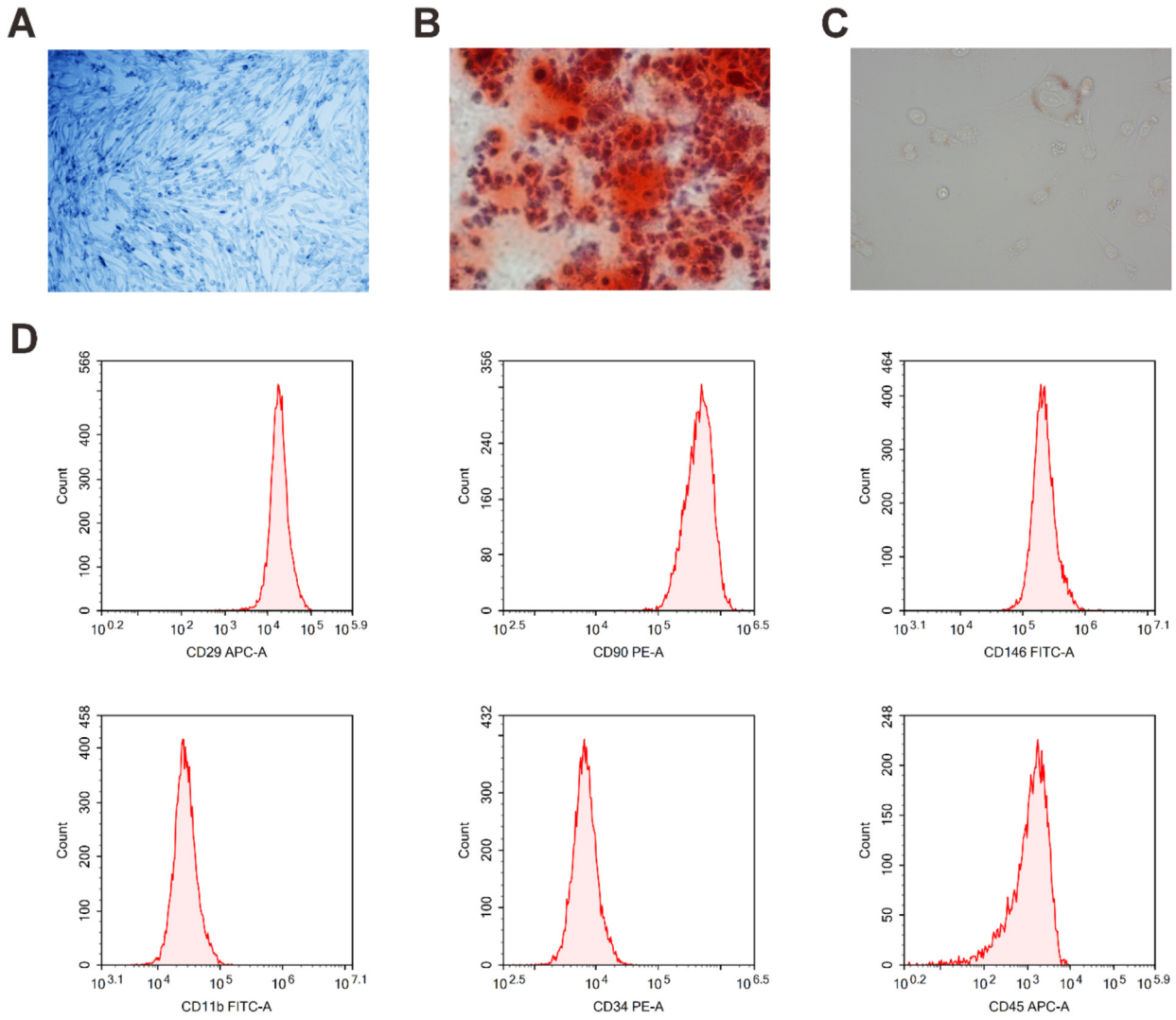

Fig. 1. Isolation and Identification of PDLSCs. (A) Cell morphology observed by methylene blue staining; (B) Osteogenic differentiation assessed by Alizarin Red S staining; (C) Adipogenic differentiation assessed by Oil Red O staining; (D) Surface marker expression of PDLSCs analyzed by flow cytometry. (For interpretation of the references to color in this figure legend, the reader is referred to the web version of this article.)

Quantitative PCR confirmed the successful incorporation of si SEMA4D and si PLXNB1 into the secreted exosomes (Fig. 4C, D). Histological assessment with H&E staining indicated enhanced bone regeneration in the alveolar defect area in groups receiving Hydrogel loaded with Exo si SEMA4D or Exo si PLXNB1, relative to the group treated with control exosomes (Fig. 4E). Correspondingly, Masson's trichrome staining showed greater collagen deposition in the defect sites of these knockdown groups (Fig. 4F). Immunohistochemical analysis revealed a further decline in iNOS positive cells and a stronger increase in CD206 positive cells following treatment with exosomes carrying si SEMA4D or si PLXNB1 (Fig. 4G, H), indicating that suppression of either SEMA4D or PLXNB1 augments the ability of PDLSCs Exo to induce M2 macrophage polarization. Moreover, ELISA results showed that serum concentrations of the pro inflammatory cytokines TNF α, IL 1β, and IL 6 were further lowered in these treatment groups (Fig. 4I, J, K).

3.5. Overexpression of SEMA4D or PLXNB1 attenuates the therapeutic effect of PDLSCs-exo on alveolar bone defect repair in periodontitis

Plasmids encoding pcDNA3.1-SEMA4D or pcDNA3.1-PLXNB1 were introduced into PDLSCs before exosome harvest. RT qPCR confirmed the efficiency of transfection and the successful packaging of these constructs into the secreted exosomes (Fig. 5A, B). H&E-stained sections demonstrated that alveolar bone defects in groups receiving Hydrogel incorporated with Exo pcDNA3.1 SEM A4D or Exo pcDNA3.1 PLXNB1 exhibited less new bone formation compared to those treated with control exosomes (Fig. 5C). Similarly, Masson's trichrome staining revealed reduced collagen deposition at the defect sites in these overexpression groups (Fig. 5D). Immunohistochemical analysis showed a higher number of iNOS positive cells and a lower number of CD206 positive cells in both the Hydrogel + Exo pcDNA3.1 SEMA4D and Hydrogel + Exo pcDNA3.1 PLXNB1 groups (Fig. 5E, F). These results imply that elevated expression of either SEMA4D or PLXNB1 compromises the ability of PDLSCs Exo to promote a shift toward the M2 macrophage phenotype. Consistent with this pro-inflammatory trend, ELISA analysis detected increased serum levels of TNF α, IL 1β, and IL 6 in these treatment groups (Fig. 5G, H, I).

3.6. SEMA4D functions through its receptor PLXNB1

To further explore the functional significance of the SEMA4D/PLXNB1 signaling axis, an *in-silico* analysis was conducted using the STRING database to predict a potential interaction between

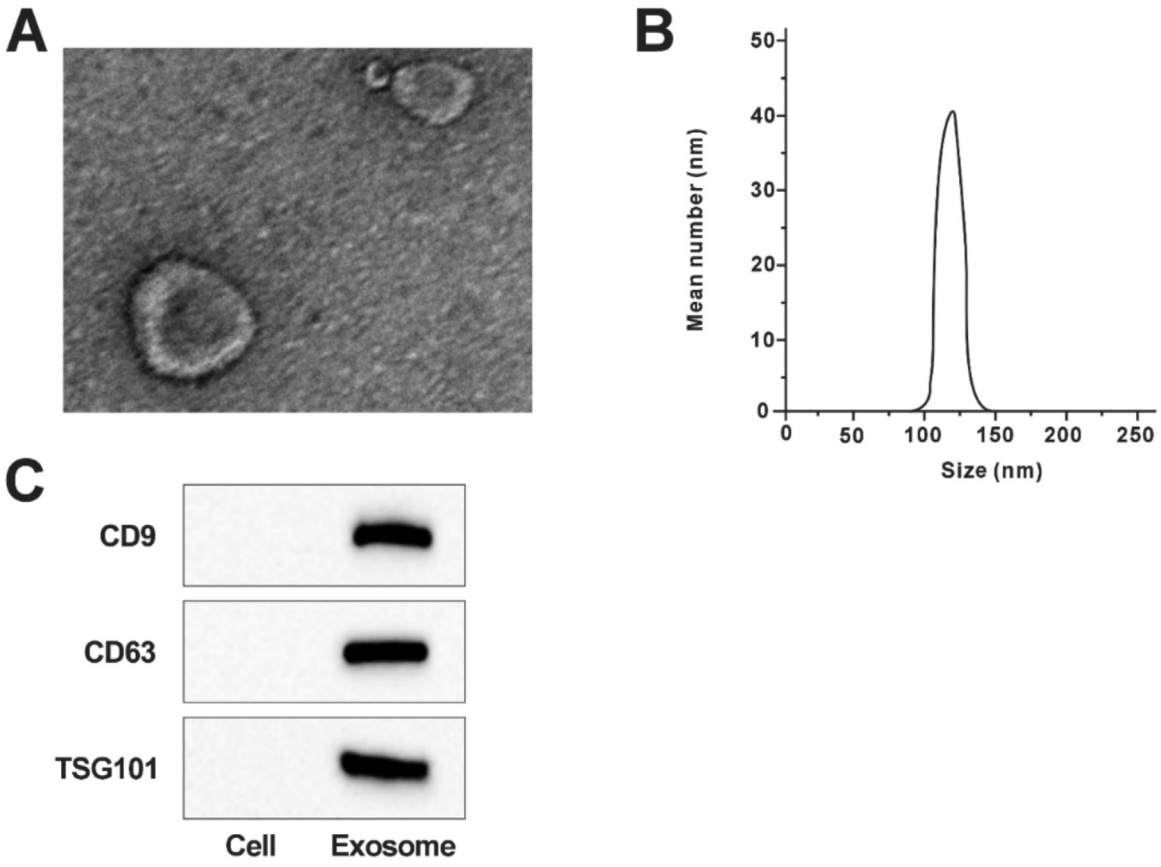

Fig. 2. Isolation and Identification of PDLSCs-Exo. (A) Exosome morphology observed by TEM; (B) Particle size distribution of exosomes analyzed by NTA; (C) Exosomal markers detected by Western blot.

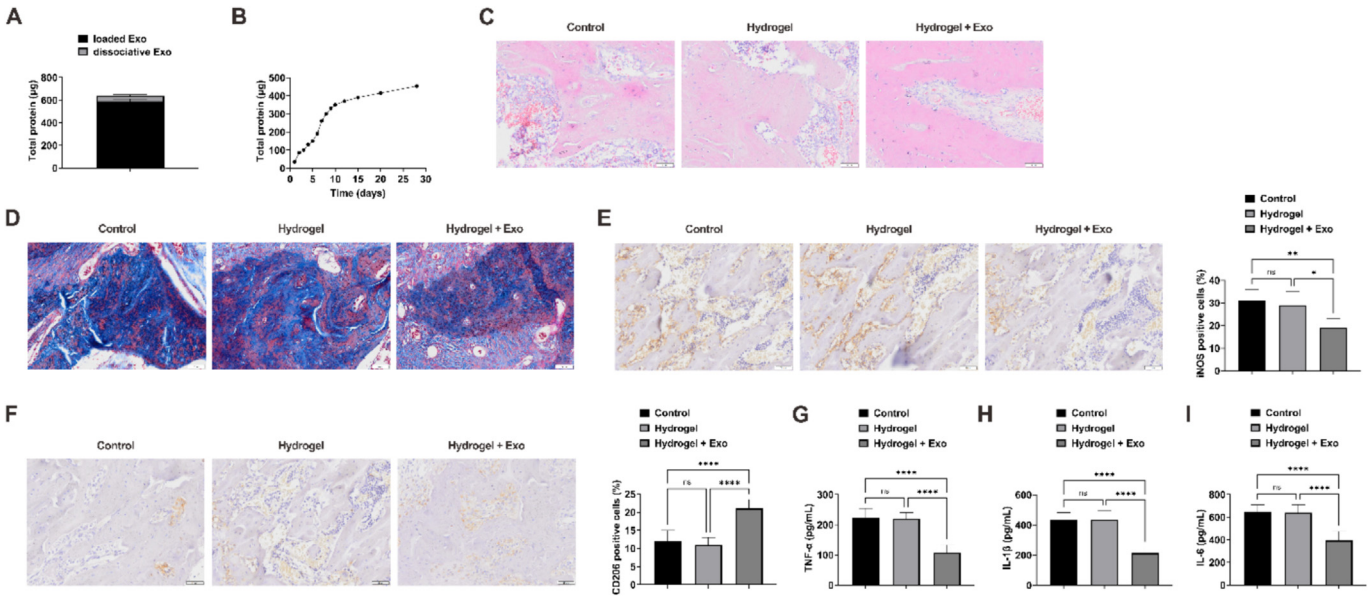

Fig. 3. PDLSCs-exo promote the repair of alveolar bone defects in periodontitis. (A, B) Exosome release assay; (C) H&E staining; (D) Masson's trichrome staining; (E, F) IHC staining of M1 (iNOS) and M2 (CD206) macrophage markers; (G, H, I) Serum levels of pro-inflammatory cytokines (TNF-α, IL-1β, and IL-6) measured by ELISA. All quantitative data are expressed as mean ± SD. * $p < 0.05$, ** $p < 0.01$, *** $p < 0.001$, **** $p < 0.0001$.

SEMA4D and PLXNB1 (Fig. 6A). This predicted interaction was then biochemically verified through co-immunoprecipitation experiments (Fig. 6B). Further functional analysis demonstrated that the concurrent overexpression of PLXNB1 counteracted the alveolar bone reparative effects achieved by SEMA4D knockdown (Fig. 6C–I).

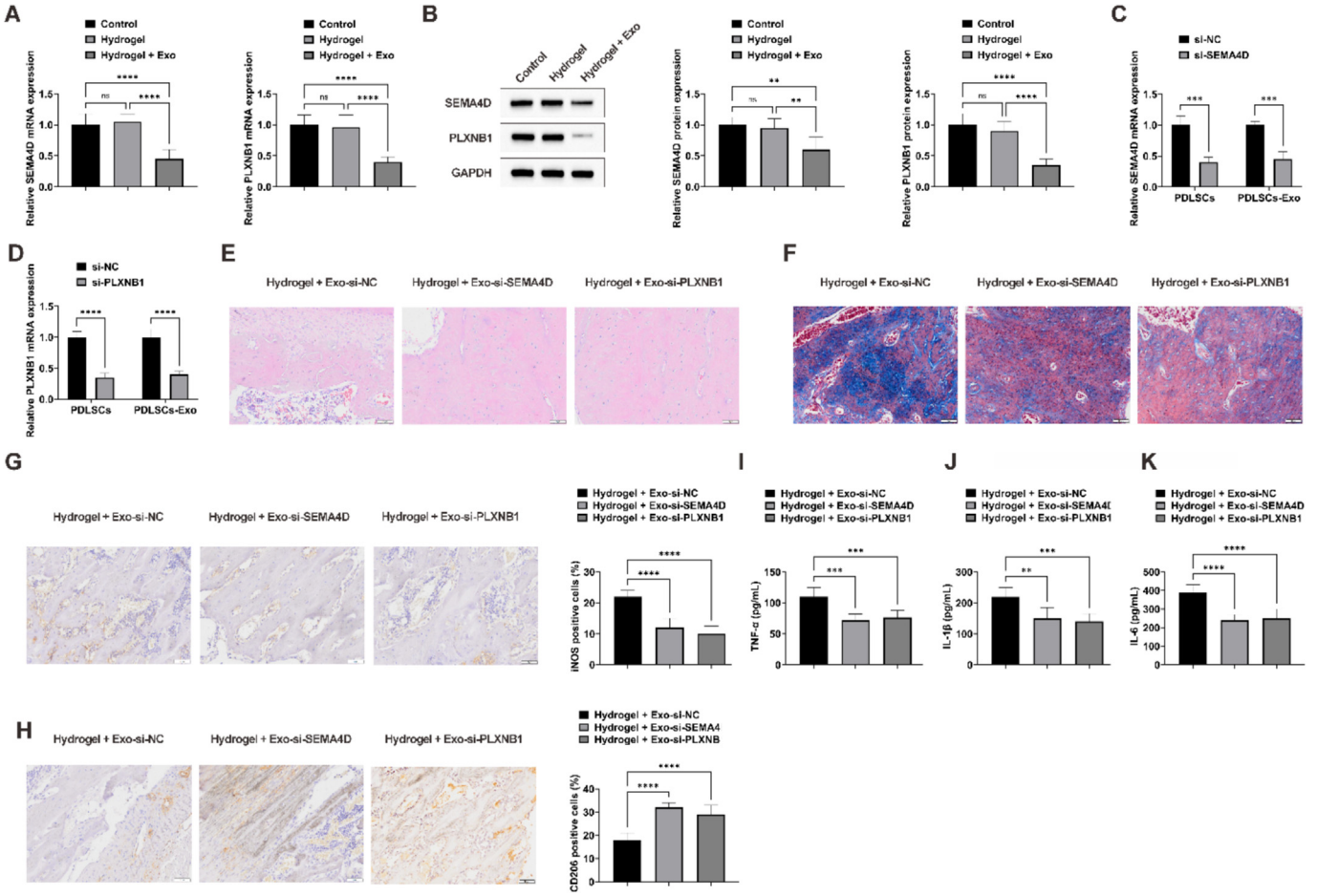

Fig. 4. Downregulation of SEMA4D or PLXNB1 enhances the therapeutic effect of PDLSCs-exo on alveolar bone defect repair in periodontitis. (A, B) Expression of SEMA4D and PLXNB1 detected by RT-qPCR and Western blot; (C, D) Transfection and packaging of si-SEMA4D or si-PLXNB1 into exosomes verified by RT-qPCR; (E) H&E staining; (F) Masson's trichrome staining; (G, H) IHC staining of M1 (iNOS) and M2 (CD206) macrophage markers; (I, J, K) Serum levels of pro-inflammatory cytokines (TNF-α, IL-1β, and IL-6) measured by ELISA. All quantitative data are expressed as mean ± SD. * $p < 0.05$, ** $p < 0.01$, *** $p < 0.001$, **** $p < 0.0001$.

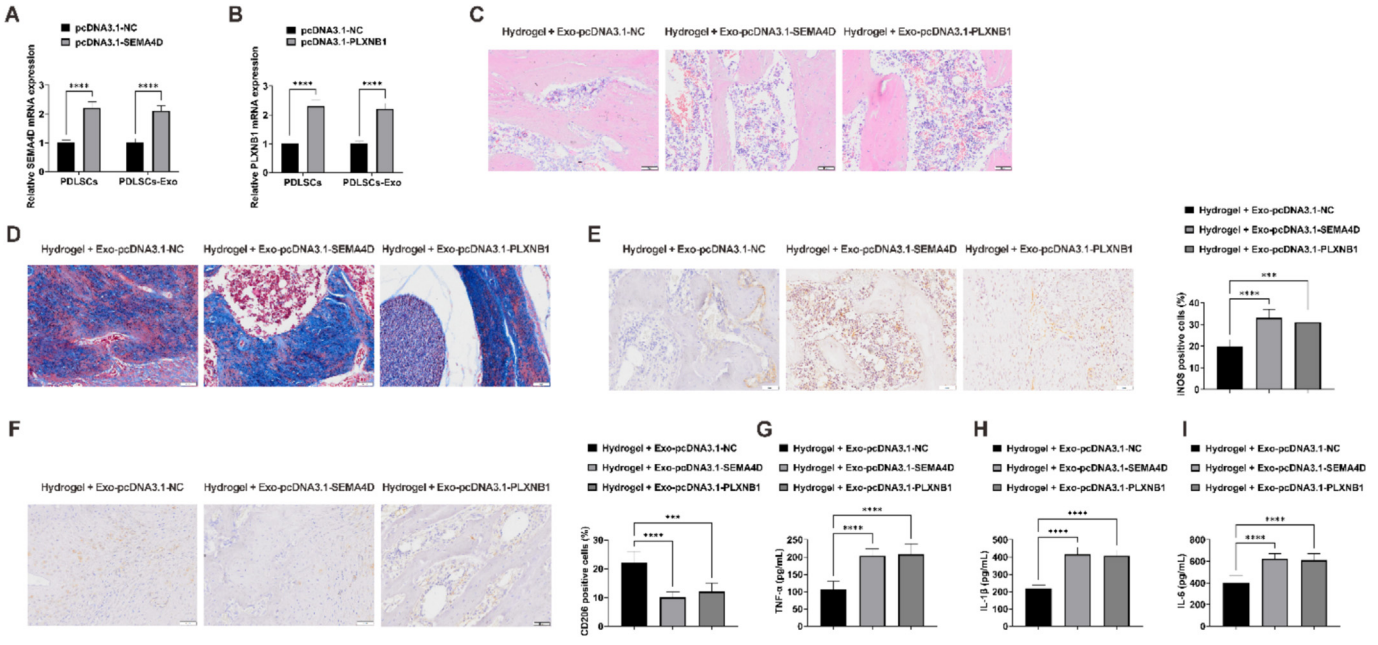

Fig. 5. Overexpression of SEMA4D or PLXNB1 attenuates the therapeutic effect of PDLSCs-exo on alveolar bone defect repair in periodontitis. (A, B) Transfection and packaging of pcDNA3.1-SEMA4D or pcDNA3.1-PLXNB1 into exosomes verified by RT-qPCR; (C) H&E staining; (D) Masson's trichrome staining; (E, F) IHC staining of M1 (iNOS) and M2 (CD206) macrophage markers; (G, H, I) Serum levels of pro-inflammatory cytokines (TNF-α, IL-1β, and IL-6) measured by ELISA. All quantitative data are expressed as mean ± SD. * $p < 0.05$, ** $p < 0.01$, *** $p < 0.001$, **** $p < 0.0001$.

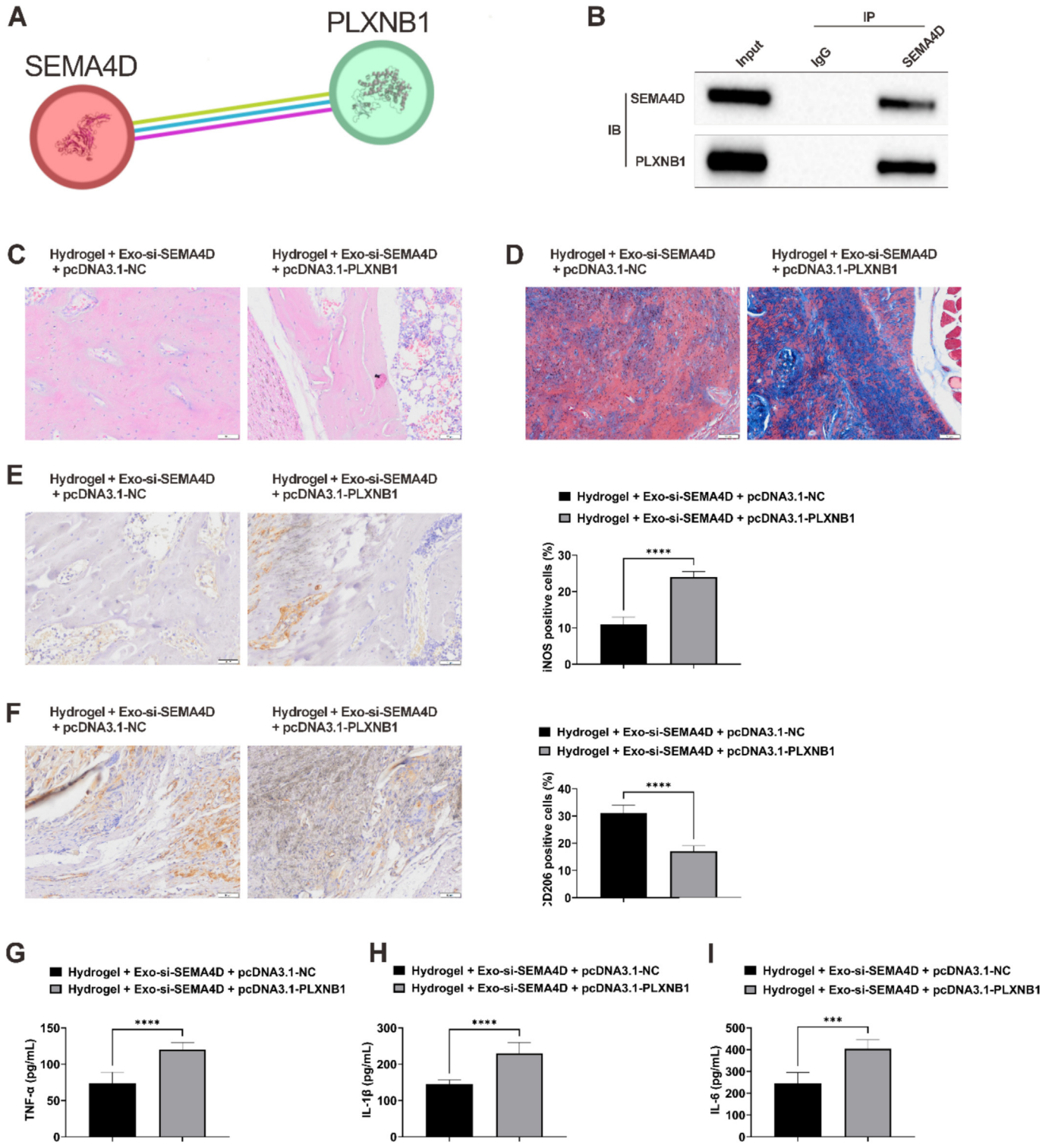

Fig. 6. SEMA4D functions through its receptor PLXNB1. (A) The interaction between SEMA4D and PLXNB1 was predicted using the STRING database; (B) The interaction was validated by Co-IP assay; (C) H&E staining; (D) Masson's trichrome staining; (E, F) IHC staining of M1 (iNOS) and M2 (CD206) macrophage markers; (G, H, I) Serum levels of pro-inflammatory cytokines (TNF-α, IL-1β, and IL-6) measured by ELISA. All quantitative data are expressed as mean ± SD. * $p < 0.05$, ** $p < 0.01$, *** $p < 0.001$, **** $p < 0.0001$.

4. Discussion

The compromised regeneration of alveolar bone in periodontitis patients is primarily driven by a combination of diminished bone-forming and blood vessel-forming abilities, persistent inflammatory overactivation, and the consequent breakdown of immune-bone equilibrium [33]. Nevertheless, existing therapeutic strategies for periodontitis fail to achieve satisfactory alveolar bone regeneration. Stem cell therapy has been demonstrated as an effective method for bone repair [37]. A number of studies have sug-

gested that the therapeutic effects of MSCs are mainly exerted through paracrine mechanisms. As key paracrine factors secreted by MSCs, exosomes hold potential applications in the field of tissue regeneration.

PDLSCs, a category of dental stem cells, are a subset of MSCs extracted from the PDL. Possessing the ability of self-renewal, they can differentiate into multiple lineages, including odontoblasts/osteoblasts, adipocytes, and neuron-like cells. In comparison with other MSCs, PDLSCs offer greater accessibility, involve fewer ethical issues, and are more economical [38]. These merits render them appropriate candidates for bone repair. Accumulating evidence has shown that exosomes derived from dental stem cells are capable of promoting tissue regeneration [39]. As a result, the present study hypothesized that PDLSCs-Exo might serve as a promising approach for repairing alveolar bone defects.

Exosomes have an unstable structure, maintaining their integrity for fewer than 48 h at room temperature [40] and even less time at 37°C. During this period, their exposed functional components (proteins and RNA) undergo rapid degradation and metabolism. To extend the retention time of PDLSCs-Exo and improve its therapeutic potential, a nanocomposite hydrogel composed of gelatin and Laponite® was employed as a delivery vehicle. Gelatin, a widely adopted biological scaffold material, is frequently used for encapsulating diverse bioactive agents [41]. Nevertheless, it exhibits limitations such as temperature sensitivity, insufficient sustained-release capacity, and poor injectability at 20°C [42]. Laponite® ((Na0.7 + [(Si8Mg5.5Li0.3)O20(OH)4]0.7-)), a synthetic nanoclay, offers favorable characteristics including a high specific surface area and net negative surface charge. These properties facilitate the adsorption of positively charged biomolecules and enable controlled release through electrostatic interactions [43,44]. Incorporating Laponite® into gelatin enhances multiple physical attributes of the hydrogel, such as improving colloidal stability and enabling better injectability. Moreover, studies have demonstrated that Laponite® contributes to the sustained release of encapsulated biological molecules, an effect that intensifies with increasing Laponite® concentration [27,45]. In this study, the nanocomposite hydrogel achieved the sustained release of PDLSCs-Exo over 28 d, confirming its role in providing controlled exosome delivery. Moreover, it was found that PDLSCs-Exo significantly promoted the formation of new bone and collagen deposition in the area of alveolar bone defects.

Macrophages constitute a pivotal immune cell subset critically involved in the pathogenesis of periodontitis, where they contribute significantly to phagocytic clearance and the regulation of immune responses. Evidence suggests that an elevated ratio of pro-inflammatory M1 macrophages is associated with intensified inflammation within periodontal tissues. These cells release cytokines such as TNF-α, IL-1β, and IL-6, which perpetuate inflammatory cascades and drive tissue degradation [46,47,48]. According to a study by Liu et al. [49], aspirin was found to inhibit M1 macrophage activation, leading to significant improvement in alveolar bone repair. In this study, PDLSCs-Exo was shown to suppress M1 macrophage polarization, promote M2 phenotype switching, and significantly reduce circulating levels of pro-inflammatory cytokines (TNF-α, IL-1β, and IL-6).

The Sema4D/Plexin B1 signaling axis, where Sema4D is secreted by osteoclasts and binds to Plexin B1 on osteoblasts, has been demonstrated to suppress osteoblast activity and bone formation [50,51,52]. In this study, PDLSC-derived exosomes were found to effectively reduce the expression levels of both SEMA4D and its receptor PLXNB1. Further experimental results demonstrated that downregulation of SEMA4D or PLXNB1 enhanced the promotive effect of PDLSCs-Exo on alveolar bone defect repair in periodontitis, while upregulation of SEMA4D or PLXNB1 attenuated this effect. Additionally, it was found that overexpression of PLXNB1 reversed the reparative benefits of SEMA4D downregulation on alveolar bone defects in periodontitis, indicating that SEMA4D functions through its receptor PLXNB1.

However, this study has several limitations. First, the molecular mechanisms through which PDLSCs-Exo modulate the expression of SEMA4D and PLXNB1 were not examined in depth. Subsequent studies ought to investigate the upstream regulatory factors of SEMA4D and PLXNB1. Additionally, even though the impact of PDLSCs-Exo on alveolar bone defect repair was assessed using a rat model of periodontitis, rodent models are unable to fully reproduce human disease states or satisfy the demands for the clinical translation of biomaterials [53]. Therefore, future investigations should incorporate large animal models to further evaluate the therapeutic effectiveness of PDLSCs-Exo in repairing alveolar bone defects associated with periodontitis.

5. Conclusions

In summary, this study demonstrates for the first time that PDLSCs-Exo facilitate M2 macrophage polarization through suppression of the SEMA4D/PLXNB1 signaling pathway, which in turn attenuates local inflammatory responses and enhances the regeneration of alveolar bone defects in a periodontitis model. This newly identified mechanism offers a promising therapeutic approach for the treatment of periodontal bone loss.

CRediT authorship contribution statement

YanZong Yang: Writing – original draft, Supervision, Resources, Methodology, Data curation, Conceptualization. **ChunBo Zhang:** Writing – review & editing, Supervision, Resources, Project administration, Investigation, Formal analysis.

Ethical approval (animals)

All animal experiments were conducted in compliance with the ARRIVE guidelines and performed in accordance with the National Institutes of Health Guide for the Care and Use of Laboratory Animals. The experiments were approved by the Institutional Animal Care and Use Committee of The First Affiliated Hospital of Xiamen University (Ethics Approval Number: D2258-4).

Financial support

This research did not receive any specific grant from funding agencies in the public, commercial, or not-for-profit sectors.

Declaration of competing interest

The authors have no conflicts of interest to declare.

Supplementary material

https://doi.org/10.1016/j.ejbt.2026.100712.

Data availability

The datasets used and/or analyzed during the present study are available from the corresponding author on reasonable request.

References

[1] Kinane DF, Stathopoulou PG, Papapanou PN. Periodontal diseases. Nat Rev Dis Primers 2017;3:17038. https://doi.org/10.1038/nrdp.2017.38. PMid: 28805207.

[2] Slots J. Periodontitis: Facts, fallacies and the future. Periodontology 2000 2017;75(1):7–23. https://doi.org/10.1111/prd.12221. PMid: 28758294.
[3] Gruber R. Osteoimmunology: Inflammatory osteolysis and regeneration of the alveolar bone. J Clin Periodontol 2019;46(S21):52–69. https://doi.org/10.1111/jcpe.13056. PMid: 30623453.
[4] Yang B, Pang X, Li Z, et al. Immunomodulation in the treatment of periodontitis: Progress and perspectives. Front Immunol 2021;12:781378. https://doi.org/10.3389/fimmu.2021.781378. PMid: 34868054.
[5] Wen Y, Yang H, Wu J, et al. COL4A2 in the tissue-specific extracellular matrix plays important role on osteogenic differentiation of periodontal ligament stem cells. Theranostics 2019;9(15):4265–86. https://doi.org/10.7150/thno.35914. PMiD: 31285761.
[6] Sufianov A, Beilerli A, Begliarzade S, et al. The role of noncoding RNAs in the osteogenic differentiation of human periodontal ligament-derived cells. Non-coding RNA Res 2023;8(1):89–95. https://doi.org/10.1016/j.ncrna.2022.11.003. PMiD: 36439972.
[7] Mantesso A, Nör JE. Stem cells in clinical dentistry. J Am Dent Assoc 2023;154(12):1048–57. https://doi.org/10.1016/j.adaj.2023.08.007. PMid: 37804275.
[8] Lei F, Li M, Lin T, et al. Treatment of inflammatory bone loss in periodontitis by stem cell-derived exosomes. Acta Biomater 2022;141:333–43. https://doi.org/10.1016/j.actbio.2021.12.035. PMid: 34979326.
[9] Chen J, Zhang G, Wan Y, et al. Immune cell-derived exosomes as promising tools for cancer therapy. J Control Release 2023;364:508–28. https://doi.org/10.1016/j.jconrel.2023.11.003. PMid: 37939852.
[10] Wang W, Liang X, Zheng K, et al. Horizon of exosome-mediated bone tissue regeneration: The all-rounder role in biomaterial engineering. Mater Today Bio 2022;16:100355. https://doi.org/10.1016/j.mtbio.2022.100355. PMid: 35875196.
[11] Xu T, Yu X, Xu K, et al. Comparison of the ability of exosomes and ectosomes derived from adipose-derived stromal cells to promote cartilage regeneration in a rat osteochondral defect model. Stem Cell Res Ther 2024;15(1):18. https://doi.org/10.1186/s13287-024-03632-4. PMid: 38229196.
[12] Miron RJ, Estrin NE, Sculean A, et al. Understanding exosomes: Part 2-Emerging leaders in regenerative medicine. Periodontology 2000 2024;94(1):257–414. https://doi.org/10.1111/prd.12561. PMid: 38591622.
[13] Zhao Y, Gong Y, Liu X, et al. The experimental study of periodontal ligament stem cells derived exosomes with hydrogel accelerating bone regeneration on alveolar bone defect. Pharmaceutics 2022;14(10):2189. https://doi.org/10.3390/pharmaceutics14102189. PMid: 36297624.
[14] Lu J, Yu N, Liu Q, et al. Periodontal ligament stem cell exosomes key to regulate periodontal regeneration by miR-31-5p in mice model. Int J Nanomed 2023;18:5327–42. https://doi.org/10.2147/IJN.S409664. PMid: 37746047.
[15] Qiao X, Tang J, Dou L, et al. Dental pulp stem cell-derived exosomes regulate anti-inflammatory and osteogenesis in periodontal ligament stem cells and promote the repair of experimental periodontitis in rats. Int J Nanomed 2023;18:4683–703. https://doi.org/10.2147/IJN.S420967. PMid: 37608819.
[16] Ahmad P, Estrin N, Farshidfar N, et al. Mechanistic insights into periodontal ligament stem cell-derived exosomes in tissue regeneration. Clin Oral Invest 2025;29(7):357. https://doi.org/10.1007/s00784-025-06422-1. PMid: 40562987.
[17] Chen L, Liu Y, Yu C, et al. Induced pluripotent stem cell-derived mesenchymal stem cells (iMSCs) inhibit M1 macrophage polarization and reduce alveolar bone loss associated with periodontitis. Stem Cell Res Ther 2025;16(1):223. https://doi.org/10.1186/s13287-025-04327-0. PMid: 40317064.
[18] Qin Z, Han Y, Du Y, et al. Bioactive materials from berberine-treated human bone marrow mesenchymal stem cells promote alveolar bone regeneration by regulating macrophage polarization. Sci China Life Sci 2024;67(5):1010–26. https://doi.org/10.1007/s11427-023-2454-9. PMid: 38489007.
[19] Kang M, Huang CC, Lu Y, et al. Bone regeneration is mediated by macrophage extracellular vesicles. Bone 2020;141:115627. https://doi.org/10.1016/j.bone.2020.115627. PMid: 32891867.
[20] Chen MH, Wang YH, Sun BJ, et al. HIF-1α activator DMOG inhibits alveolar bone resorption in murine periodontitis by regulating macrophage polarization. Int Immunopharmacol 2021;99:107901. https://doi.org/10.1016/j.intimp.2021.107901. PMid: 34273637.
[21] Li Y, Liu L, Li Y, et al. Alpha-ketoglutarate promotes alveolar bone regeneration by modulating M2 macrophage polarization. Bone Rep 2023;18:101671. https://doi.org/10.1016/j.bonr.2023.101671. PMid: 37007218.
[22] Qiao D, Cheng S, Song S, et al. Polarized M2 macrophages induced by glycosylated nano-hydroxyapatites activate bone regeneration in periodontitis therapy. J Clin Periodontol 2024;51(8):1054–65. https://doi.org/10.1111/jcpe.13999. PMid: 38736143.
[23] Zhang Y, Wei L, Miron RJ, et al. Anabolic bone formation via a site-specific bone-targeting delivery system by interfering with semaphorin 4D expression. J Bone Miner Res 2015;30(2):286–96. https://doi.org/10.1002/jbmr.2322. PMid: 25088728.
[24] Seo BM, Miura M, Gronthos S, et al. Investigation of multipotent postnatal stem cells from human periodontal ligament. Lancet 2004;364(9429):149–55. https://doi.org/10.1016/S0140-6736(04)16627-0. PMid: 15246727.
[25] Zhang Y, Kong N, Zhang Y, et al. Size-dependent effects of gold nanoparticles on osteogenic differentiation of human periodontal ligament progenitor cells. Theranostics 2017;7(5):1214–24. https://doi.org/10.7150/thno.17252. PMid: 28435460.
[26] Liu M, Chen R, Xu Y, et al. Exosomal miR-141-3p from PDLSCs alleviates high glucose-induced senescence of PDLSCs by activating the KEAP1-NRF2 signaling pathway. Stem Cells Int 2023;2023:7136819. https://doi.org/10.1155/2023/7136819. PMid: 37274022.
[27] Waters R, Alam P, Pacelli S, et al. Stem cell-inspired secretome-rich injectable hydrogel to repair injured cardiac tissue. Acta Biomater 2018;69:95–106. https://doi.org/10.1016/j.actbio.2017.12.025. PMid: 29281806.
[28] Konečná B, Chobodová P, Janko J, et al. The effect of melatonin on periodontitis. Int J Mol Sci 2021;22(5):2390. https://doi.org/10.3390/ijms22052390. PMid: 33673616.
[29] Bhattarai G, Poudel SB, Kook SH, et al. Resveratrol prevents alveolar bone loss in an experimental rat model of periodontitis. Acta Biomater 2016;29:398–408. https://doi.org/10.1016/j.actbio.2015.10.031. PMid: 26497626.
[30] Lin P, Niimi H, Ohsugi Y, et al. Application of ligature-induced periodontitis in mice to explore the molecular mechanism of periodontal disease. Int J Mol Sci 2021;22(16):8900. https://doi.org/10.3390/ijms22168900. PMid: 34445604.
[31] de Molon RS, Park CH, Jin Q, et al. Characterization of ligature-induced experimental periodontitis. Microscopy Research & Technique 2018;81(12):1412–21. https://doi.org/10.1002/jemt.23101. PMid: 30351474.
[32] Zhang C, Li T, Zhou C, et al. Parathyroid hormone increases alveolar bone homoeostasis during orthodontic tooth movement in rats with periodontitis via crosstalk between STAT3 and β-catenin. Int J Oral Sci 2020;12(1):38. https://doi.org/10.1038/s41368-020-00104-2. PMid: 33380723.
[33] Yang SY, Hu Y, Zhao R, et al. Quercetin-loaded mesoporous nano-delivery system remodels osteoimmune microenvironment to regenerate alveolar bone in periodontitis via the miR-21a-5p/PDCD4/NF-κB pathway. J Nanobiotechnol 2024;22(1):94. https://doi.org/10.1186/s12951-024-02352-4. PMid: 38449005.
[34] Xu W, Tan W, Li C, et al. Metformin-loaded β-TCP/CTS/SBA-15 composite scaffolds promote alveolar bone regeneration in a rat model of periodontitis. J Mater Sci Mater Med 2021;32(12):145. https://doi.org/10.1007/s10856-021-06621-8. PMid: 34862928.
[35] Luo H, Chen D, Li R, et al. Genetically engineered CXCR4-modified exosomes for delivery of miR-126 mimics to macrophages alleviate periodontitis. J Nanobiotechnol 2023;21(1):116. https://doi.org/10.1186/s12951-023-01863-w. PMid: 36991451.
[36] Kaneda T, Miyauchi M, Takekoshi T, et al. Characteristics of periodontal ligament subpopulations obtained by sequential enzymatic digestion of rat molar periodontal ligament. Bone 2006;38(3):420–6. https://doi.org/10.1016/j.bone.2005.08.021. PMid: 16243014.
[37] Hao ZC, Lu J, Wang SZ, et al. Stem cell-derived exosomes: A promising strategy for fracture healing. Cell Prolif 2017;50(5):e12359. https://doi.org/10.1111/cpr.12359. PMid: 28741758.
[38] Tomokiyo A, Wada N, Maeda H. Periodontal ligament stem cells: Regenerative potency in periodontium. Stem Cells Dev 2019;28(15):974–85. https://doi.org/10.1089/scd.2019.0031. PMid: 31215350.
[39] Hu X, Zhong Y, Kong Y, et al. Lineage-specific exosomes promote the odontogenic differentiation of human dental pulp stem cells (DPSCs) through TGFβ1/smads signaling pathway via transfer of microRNAs. Stem Cell Res Ther 2019;10(1):170. https://doi.org/10.1186/s13287-019-1278-x. PMid: 31196201.
[40] Chew JRJ, Chuah SJ, Teo KYW, et al. Mesenchymal stem cell exosomes enhance periodontal ligament cell functions and promote periodontal regeneration. Acta Biomater 2019;89:252–64. https://doi.org/10.1016/j.actbio.2019.03.021. PMid: 30878447.
[41] Wang H, Zou Q, Boerman OC, et al. Combined delivery of BMP-2 and bFGF from nanostructured colloidal gelatin gels and its effect on bone regeneration *in vivo*. J Control Release 2013;166(2):172–81. https://doi.org/10.1016/j.jconrel.2012.12.015. PMid: 23266450.
[42] Gnavi S, di Blasio L, Tonda-Turo C, et al. Gelatin-based hydrogel for vascular endothelial growth factor release in peripheral nerve tissue engineering. J Tissue Eng Regen Med 2017;11(2):459–70. https://doi.org/10.1002/term.1936. PMid: 24945739.
[43] Tous E, Purcell B, Ifkovits JL, et al. Injectable acellular hydrogels for cardiac repair. J Cardiovasc Transl Res 2011;4(5):528–42. https://doi.org/10.1007/s12265-011-9291-1. PMid: 21710332.
[44] Liu L, Guo S, Shi W, et al. Bone marrow mesenchymal stem cell-derived small extracellular vesicles promote periodontal regeneration. Tissue Eng A 2021;27(13–14):962–76. https://doi.org/10.1089/ten.TEA.2020.0141. PMid: 32962564.
[45] Ding X, Gao J, Wang Z, et al. A shear-thinning hydrogel that extends *in vivo* bioactivity of FGF2. Biomaterials 2016;111:80–9. https://doi.org/10.1016/j.biomaterials.2016.09.026. PMid: 27728816.
[46] Yin L, Li X, Hou J. Macrophages in periodontitis: A dynamic shift between tissue destruction and repair. Japanese Dental Science Review 2022;58:336–47. https://doi.org/10.1016/j.jdsr.2022.10.002. PMid: 36340583.
[47] Guo X, Wu Z. GABARAP ameliorates IL-1β-induced inflammatory responses and osteogenic differentiation in bone marrow-derived stromal cells by activating autophagy. Sci Rep 2021;11(1):11561. https://doi.org/10.1038/s41598-021-90586-9. PMid: 34078931.
[48] Wimalawansa SJ. Nitric oxide and bone. Ann N Y Acad Sci 2010;1192(1):391–403. https://doi.org/10.1111/j.1749-6632.2009.05230.x. PMid: 20392265.
[49] Liu Y, Fang S, Li X, et al. Aspirin inhibits LPS-induced macrophage activation *via* the NF-κB pathway. Sci Rep 2017;7(1):11549. https://doi.org/10.1038/s41598-017-10720-4. PMid: 28912509.

[50] Terpos E, Ntanasis-Stathopoulos I, Christoulas D, et al. Semaphorin 4D correlates with increased bone resorption, hypercalcemia, and disease stage in newly diagnosed patients with multiple myeloma. Blood Cancer J 2018;8 (5):42. https://doi.org/10.1038/s41408-018-0075-6. PMid: 29748532.
[51] Deb Roy A, Yin T, Choudhary S, et al. Optogenetic activation of Plexin-B1 reveals contact repulsion between osteoclasts and osteoblasts. Nat Commun 2017;8:15831. https://doi.org/10.1038/ncomms15831. PMid: 28635959.
[52] Negishi-Koga T, Shinohara M, Komatsu N, et al. Suppression of bone formation by osteoclastic expression of semaphorin 4D. Nat Med 2011;17(11):1473–80. https://doi.org/10.1038/nm.2489. PMid: 22019888.
[53] Gui Q, Lyons DJ, Deeb JG, et al. Non-human primate *Macaca mulatta* as an animal model for testing efficacy of amixicile as a targeted anti-periodontitis therapy. Front Oral Health 2021;2:752929. https://doi.org/10.3389/froh.2021.752929. PMid: 35048063.